

Article

Single-Spin Asymmetry of Neutrons in Polarized pA Collisions

Boris Z. Kopeliovich ^{*}, Irina K. Potashnikova and Iván Schmidt 

Departamento de Física, Universidad Técnica Federico Santa María, Avenida España 1680, Valparaíso 239-0123, Chile; irina.potashnikova@usm.cl (I.K.P.); ivan.schmidt@usm.cl (I.S.)

^{*} Correspondence: boris.kopeliovich@usm.cl

Abstract: Absorptive corrections, which are known to suppress proton-neutron transitions with a large fractional momentum $z \rightarrow 1$ in pp collisions, become dramatically strong on a nuclear target, and they push the partial cross sections of leading neutron production to the very periphery of the nucleus. The mechanism of the pion π and axial vector meson a_1 interference, which successfully explains the observed single-spin asymmetry in a polarized $pp \rightarrow nX$, is extended to the collisions of polarized protons with nuclei. When corrected for nuclear effects, it explains the observed single-spin azimuthal asymmetry of neutrons that is produced in inelastic events, which is where the nucleus violently breaks up. This single-spin asymmetry is found to be negative and nearly atomic mass number A -independent.

Keywords: neutron production; pion pole; interference; spin-flip; azimuthal asymmetry

1. Proton-Neutron Transitions in the Vicinity of the Pion Pole

The pion is known to have a large coupling to nucleons; therefore, pion exchange is important in processes with isospin one in the cross channel (e.g., $p + n \rightarrow n + p$). However, the Regge pion trajectory has a low intercept of $\alpha_\pi(0) \approx 0$, and this is why it ceases to be important at high energies in binary reactions. Meanwhile, other mesons, such as ρ , a_2 , etc., take over. More specifically, in the inclusive production of neutrons, the whole rapidity interval is divided between the rapidity gap and the excited multiparticle state X with invariant mass. The latter might be sufficiently large enough to reduce the rapidity gap, i.e., what allows pion exchange.

2. A Triple-Regge Description of Neutron Production

The process $p \uparrow + p(A) \rightarrow n + X$ that has a large, fractional light-cone momentum $z = p_n^+ / p_p^+$ of neutrons produced that is in the proton beam direction (rather, in the target direction, i.e., the asymmetry is zero according to the Abarbanel-Gross theorem [1]), is known to be related to the iso-vector Reggeons (π , ρ , a_2 , a_1 , etc.) [2]. Here, the upward arrow denotes that the proton is transversely polarized, and the '+' sign denotes the plus-component of the particle light-cone momentum. As illustrated in Figure 1, the amplitude, squared, and summed over values of the final states X (at a fixed invariant mass, M_X) are expressed via the Reggeon-proton total cross section at the centre-of-mass (c.m.) energy M_X .

$$\sum_X \left| \frac{p \quad n}{\quad \quad} \right|^2 = \frac{p \quad n \quad n \quad p}{\quad \quad} = \frac{p \quad p}{\quad \quad} \sigma_{\text{tot}}^{pR}(M_X^2)$$

Figure 1. Graphical relation between the cross section of neutron production and the total Reggeon-proton cross section, σ_{tot}^{pR} , which—when with a large invariant mass, M_X^2 , of the final states—is dominated by the Pomeron, \mathbb{P} .



Citation: Kopeliovich, B.Z.;

Potashnikova, I.K.; Schmidt, I.

Single-Spin Asymmetry of Neutrons in Polarized pA Collisions. *Physics* 2023, 5, 1048–1060. <https://doi.org/10.3390/physics5040068>

Received: 11 September 2023

Revised: 12 October 2023

Accepted: 19 October 2023

Published: 7 November 2023



Copyright: © 2023 by the authors. Licensee MDPI, Basel, Switzerland. This article is an open access article distributed under the terms and conditions of the Creative Commons Attribution (CC BY) license (<https://creativecommons.org/licenses/by/4.0/>).

At high energies of colliders (RHIC (Relativistic Heavy Ion Collider), LHC (Large Hadron Collider) and others), the $M_X^2 = s(1 - z)$, where s denotes the collision c.m. energy squared, is so large (except in the inaccessibly small $1 - z$) that the cross section $\sigma_{\text{tot}}^{pR}(M_X^2)$ is dominated by the Pomeron exchange, as is illustrated in Figure 1. The couplings of the iso-vector Reggeons, specifically those with a natural parity (ρ, a_2) with the proton, are known to be predominantly spin-flip [3]; as such, they can be neglected, and this is the case because we are interested here in the small transverse momenta, $p_T \rightarrow 0$, of the neutrons. Only unnatural parity Reggeons (π, a_1) have large spin non-flip couplings that contribute in the forward direction.

3. Cross Section of Forward Neutron Production

3.1. Pion Pole

Pions are known to have a large coupling with nucleons; thus, the pion exchange is important in processes with isospin flip, like in $p \rightarrow n$. Measurements with polarized proton beams supply more detailed information about the interaction dynamic. The cross section of neutron production in the vicinity of the pion pole was measured at the ISR (the Interacting Storage Rings) in pp collisions [4] and in deep inelastic scattering (DIS) at HERA (Hadron-Electron Ring Accelerator) [5]. The cross section has also been calculated within various theoretical schemes [6–12].

The pion term in the cross section of neutron production reads as follows [2]:

$$z \frac{d\sigma^B(pp \rightarrow nX)}{dz dq_T^2} \Big|_{\pi} = f_{\pi/p}(z, q_T, q_L) \sigma_{\text{tot}}^{\pi^+p}(s'). \tag{1}$$

Here, z is related to M_X and $z \approx 1 - M_X^2/s$ for $1 - z \ll 1$, where \sqrt{s} is the c.m. energy of pp collision. Furthermore, $s' = M_X^2$ and the superscript B means that this is a Born approximation; thus, the absorptive corrections will be ignored and considered later on.

$f_{\pi/p}(z, q_T, q_L)$ is the pion flux in the proton, and it has the form

$$f_{\pi/p}(z, q_T, q_L) = |t| G_{\pi^+pn}^2(t) |\eta_{\pi}(t)|^2 \left(\frac{\alpha'_{\pi}}{8}\right)^2 \times (1 - z)^{1-2\alpha_{\pi}(t)}. \tag{2}$$

Here, q_T is the neutron transverse momentum, $q_L = m_N(1 - z)/\sqrt{z}$, with m_N denoting the nucleon mass, $-t = q_L^2 + q_T^2/z$, α'_{π} is the slope of the pion Regge trajectory, and $G_{\pi^+pn}(t)$ is the effective πN vertex function [2,5]. $G_{\pi^+pn}(t) = g_{\pi^+pn} \exp(R_{\pi NN}^2 t)$ includes the pion-nucleon coupling and the form factor which incorporates the t -dependence of the coupling and of the πN inelastic amplitude. We take the values of the parameters used in Ref. [5] $g_{\pi^+pn}^2/8\pi = 13.85$ and $R_{\pi NN}^2 = 0.3 \text{ GeV}^{-2}$. Notice that the choice of $R_{\pi NN}$ does not bring much uncertainty, since we focus here at data for forward production, $q_T = 0$, so t is quite small. The signature factor is $\eta_{\pi}(t) = i - \cot[\pi\alpha_{\pi}(t)/2]$.

The amplitude of the process includes both non-flip and spin-flip terms as follows [2,13]:

$$A_{p \rightarrow n}^B(\vec{q}, z) = \bar{\zeta}_n \left[\sigma_3 q_L + \frac{1}{\sqrt{z}} \vec{\sigma} \cdot \vec{q}_T \right] \zeta_p \phi^B(q_T, z), \tag{3}$$

where $\vec{\sigma}$ are the Pauli matrices, and $\zeta_{p,n}$ are the proton or neutron spinors.

In the region of a small $1 - z \ll 1$, the pseudo-scalar amplitude $\phi^B(q_T, z)$ has the triple-Regge form (see Figure 1) as follows:

$$\phi^B(q_T, z) = \frac{\alpha'_{\pi}}{8} G_{\pi^+pn}(t) \eta_{\pi}(t) (1 - z)^{-\alpha_{\pi}(t)} \times A_{\pi p \rightarrow X}(M_X^2). \tag{4}$$

The procedure of inclusion of the absorptive corrections on the amplitude level was developed in Refs. [2,14]. First, the amplitude (3) is Fourier transformed to impact parameter representation, which is where the absorptive effect is just a multiplicative suppression factor. Then, the absorption-corrected amplitude is Fourier transformed back to a momentum representation. The effects of absorption turn out to be quite strong, i.e., it roughly reduces the neutron production cross section two-fold, and it differently affects the non-flip and spin-flip terms in the amplitude. Details of the calculations can be found in Refs. [2,14,15].

Notice that the contributions of other iso-vector Reggeons, such as ρ , a_2 , and the effective \tilde{a}_1 were calculated in Ref. [14]. For the kinematics of data under discussion [16], $q_T^2 \sim 0.01 \text{ GeV}^2$, $\langle z \rangle = 0.75$, ρ , and a_2 were found to be vanishingly small (see Figure 8 in Ref. [14]). The contribution of \tilde{a}_1 was small as well, but it did not contribute to the single-spin asymmetry.

There was also a contribution of neutrons to the production and decay of Δ resonance as well as to other resonances. This phenomenon was carefully evaluated in Ref. [5], whereby the results of a phase-shift analysis of πN was employed by scattering at low energies. This correction was also found to be small in Ref. [5]. Therefore, the dominance of the pion is well justified.

3.2. Absorptive Corrections

Like any process with LRGs, forward neutron production is subject to the large absorptive corrections that come from initial/final state interactions, as illustrated in Figure 2.

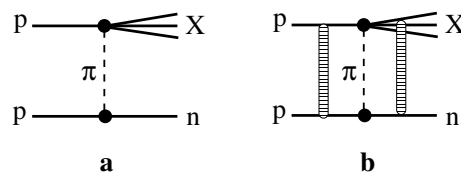


Figure 2. Graphical illustration of the absorptive effects in inclusive neutron production in proton-proton collisions: (a) the pion exchange (dashed line) in the Born approximation; (b) absorptive corrections due to initial and final state interactions shown by ladder-type exchanges.

The evaluation of the corrections is quite complicated in momentum representation, i.e., where they require multi-loop integrations. However, if these corrections do not correlate with the amplitude of the process $\pi^+ p \rightarrow X$, then they factorize in impact parameters and become much simpler. Therefore, first of all, one should Fourier transform the amplitude Equation (3) to impact the parameter space.

The partial Born amplitude at impact parameter \vec{b} , which corresponds to Equation (1) for the differential cross section, has the form [2]

$$f_{p \rightarrow n}^B(\vec{b}, z) = \frac{1}{\sqrt{z}} \bar{\zeta}_n \left[\sigma_3 \tilde{q}_L \theta_0^B(b, z) - i \frac{\vec{\sigma} \cdot \vec{b}}{b} \theta_s^B(b, z) \right] \zeta_p, \tag{5}$$

where

$$\begin{aligned} \theta_0^B(b, z) &= \int d^2q e^{i\vec{b}\vec{q}} \phi^B(q_T, z) \\ &= \frac{N(z)}{1 - \beta^2 \epsilon^2} [K_0(\epsilon b) - K_0(b/\beta)], \end{aligned} \tag{6}$$

$$\begin{aligned} \theta_s^B(b, z) &= \frac{1}{b} \int d^2q e^{i\vec{b}\vec{q}} (\vec{b} \cdot \vec{q}) \phi^B(q_T, z) \\ &= \frac{N(z)}{1 - \beta^2 \epsilon^2} \left[\epsilon K_1(\epsilon b) - \frac{1}{\beta} K_1(b/\beta) \right]. \end{aligned} \tag{7}$$

Here, $K_{0,1}$ are the modified Bessel functions of the zero and first orders, respectively, and

$$\begin{aligned}
 N(z) &= \frac{1}{2} g_{\pi+p} z(1-z)^{\alpha'_\pi(m_\pi^2 + \tilde{q}_L^2/z)} e^{-R_{\pi NN}^2 \tilde{q}_L^2/z} \\
 &\times A_{\pi p \rightarrow X}(M_X^2) \\
 e^2 &= \tilde{q}_L^2 + z m_\pi^2, \\
 \beta^2 &= R_{\pi NN}^2 - \alpha'_\pi \frac{\ln(1-z)}{z}.
 \end{aligned}
 \tag{8}$$

To simplify the calculations we replaced here, the Gaussian form factor $\exp(-\beta^2 q_T^2)$ is replaced with the monopole form $1/(1 + \beta^2 q_T^2)$, which is a suitable approximation of the small values of q_T that we are interested in.

The corrected cross section is then calculated as a convolution of the cross section with the survival probability amplitude factor:

$$f_{p \rightarrow n}(b, z) = f_{p \rightarrow n}^B(b, z) S(b, z),
 \tag{9}$$

where $S(b, z)$ is the survival amplitude.

The process under consideration, i.e., that the large $z \rightarrow 1$ is associated with the creation of a large rapidity gap (LRG) $\Delta y = |\ln(1-z)|$, which is where no particle is produced. Absorptive corrections may be also interpreted as a suppression that is related to the survival probability of LRG.

The process under consideration contains the amplitude of the pion-proton inelastic collision $\pi + p \rightarrow X$. The latter is typically described as a color exchange that leads to the creation of two color octet states with a large rapidity interval $\sim \ln(M_X^2/s_0)$ ($s_0 = 1 \text{ GeV}^2$). Perturbatively, the interaction is mediated by gluonic exchanges. Nonperturbatively, e.g., in the string model, the hadron collision looks like there is a crossing and flip of the strings.

One may think that this is the produced color octet-octet state, which experiences the final state interactions with the recoil neutron. On the other hand, at high energies, multiple interactions become coherent, and both initial and final state interactions must be included. This leads to a specific space-time development of the process at high energies; namely, the incoming proton fluctuates into a five-quark state, $|\{3q\}_8\{\bar{q}q\}_8\rangle$, which is long, in advance, in its interaction with the target via pion exchange.

We evaluate $S(b, z)$ with the color dipole model. One can present the survival amplitude of a five-quark state with an accuracy of $1/N_c^2$ as

$$S^{(5q)}(b) = S^{(3q)}(b) S^{(q\bar{q})}(b) = \left[1 - \text{Im} \Gamma^{(3q)p}(b)\right] \left[1 - \text{Im} \Gamma^{(\bar{q}q)p}(b)\right].
 \tag{10}$$

The elastic amplitude $\Gamma^{(\bar{3}3)p}(b)$ of a color $\{\bar{3}3\}$ dipole interacting with a proton is related to the partial elastic amplitude [2],

$$\text{Im} \Gamma^{(\bar{3}3)p}(b, z) = \int d^2r W_{\bar{3}3}(r, M_X^2) \text{Im} f_{\text{el}}^{\bar{3}3}(\vec{b}, \vec{r}, s, \alpha),
 \tag{11}$$

where α is the fractional light-cone momentum carried by the 3 or $\bar{3}$ triplets, r is the dipole transverse size and $W_{\bar{3}3}(r, M_X^2)$ is the dipole size distribution function [2].

4. Azimuthal Asymmetry of Neutrons in pp Collisions

4.1. Born Approximation

Both terms in the amplitude (3) have the same phase factor, $\eta_\pi(t)$. Therefore, in spite of the presence of both spin-flip and non-flip amplitudes, no single-spin asymmetry associated with pion exchange is possible in the Born approximation. Even the inclusion of absorptive corrections leave the spin effects miserably small [13,17] compared to the data [18,19].

A plausible candidate for generating a sizable spin asymmetry at high energies is the a_1 meson exchange since a_1 can be produced by pions diffractively. However, this axial-

vector resonance is hardly visible in the diffractive channels $\pi + p \rightarrow 3\pi + p$, which are dominated by $\pi\rho$ in the 1^+S wave. The $\pi\rho$ invariant mass distribution forms a pronounced narrow peak at the invariant mass $M_{\pi\rho} \approx m_{a_1}$ (due to the Deck effect [20]). Although, in the dispersion relation for the amplitude, this channel corresponds to a cut, it can be replaced with good accuracy by an effective pole \tilde{a}_1 [13,21]. In the crossed channel, $\pi\rho$ exchange corresponds to a Regge cut with the known intercept and slope of the Regge trajectory [13].

The expression for the single-spin asymmetry arises from the $\pi \tilde{a}_1$ interference, which has the form [13]

$$A_N^{(\pi \tilde{a}_1)}(q_T, z) = q_T \frac{4m_N q_L}{|t|^{3/2}} (1-z)^{\alpha_\pi(t) - \alpha_{\tilde{a}_1}(t)} \tag{12}$$

$$\times \frac{\text{Im} \eta_\pi^*(t) \eta_{\tilde{a}_1}(t)}{|\eta_\pi(t)|^2} \left(\frac{d\sigma_{\pi p \rightarrow \tilde{a}_1 p}(M_X^2)/dt|_{t=0}}{d\sigma_{\pi p \rightarrow \pi p}(M_X^2)/dt|_{t=0}} \right)^{1/2} \frac{g_{\tilde{a}_1^+ pn}}{g_{\pi^+ pn}}.$$

The trajectory of the $\pi\rho$ Regge cut and the phase factor $\eta_{\tilde{a}_1}(t)$ are known from Regge phenomenology. The $\tilde{a}_1 NN$ coupling was evaluated in Ref. [13], and it is based on the partial conservation of axial current (PCAC) and the second Weinberg sum rule, where the spectral functions of the vector and axial currents are represented by the ρ and the effective \tilde{a}_1 poles, respectively. This leads to the following relations between the couplings:

$$\frac{g_{\tilde{a}_1 NN}}{g_{\pi NN}} = \frac{m_{\tilde{a}_1}^2 f_\pi}{2m_N f_\rho} \approx \frac{1}{2}, \tag{13}$$

where $f_\pi = 0.93m_\pi$ is the pion decay coupling, $f_\rho = \sqrt{2}m_\rho^2/\gamma_\rho$ and γ_ρ is the universal coupling: $\gamma_\rho^2/4\pi = 2.4$.

4.2. Absorption-Corrected Spin Amplitudes

The absorption corrections to the spin amplitudes in Equation (5) with respect to the impact parameter representation are calculated in analogy to Equation (9):

$$\tilde{\theta}_{0,s}(b, z) = \theta_{0,s}^B(b, z) S_{0,s}(b, z), \tag{14}$$

where the absorption factors $S_{0,s}(b, z)$ are different for the spin amplitudes, as is explained and evaluated in Ref. [2].

By performing an inverse Fourier transformation back to momentum representation, one obtains the absorption-corrected spin amplitudes

$$A_{p \rightarrow n}(\vec{q}, z) = \bar{\xi}_n \left[\sigma_3 q_L \phi_0(q_T, z) - i \vec{\sigma} \cdot \vec{q}_T \frac{\phi_s(q_T, z)}{\sqrt{z}} \right] \xi_p, \tag{15}$$

where the amplitudes $\phi_{0,s}$ are given by the inverse Fourier transformation back to momentum representation:

$$\text{Re} \phi_0(q_T, z) = \frac{N(z)}{2\pi(1-\beta^2\epsilon^2)} \int_0^\infty db b J_0(bq_T) \left[K_0(\epsilon b) - K_0\left(\frac{b}{\beta}\right) \right] S(b, z),$$

$$\text{Im} \phi_0(q_T, z) = \frac{\alpha'_\pi N(z)}{4z\beta^2} \int_0^\infty db b J_0(bq_T) K_0\left(\frac{b}{\beta}\right) S(b, z), \tag{16}$$

$$\begin{aligned}
 q_T \operatorname{Re} \phi_s(q_T, z) &= \frac{N(z)}{2\pi(1-\beta^2\epsilon^2)} \int_0^\infty db b J_1(bq_T) \left[\epsilon K_1(\epsilon b) - \frac{1}{\beta} K_1\left(\frac{b}{\beta}\right) \right] S(b, z), \\
 q_T \operatorname{Im} \phi_0(q_T, z) &= \frac{\alpha'_\pi N(z)}{4z\beta^3} \int_0^\infty db b J_1(bq_T) K_1\left(\frac{b}{\beta}\right) S(b, z).
 \end{aligned}
 \tag{17}$$

Here $J_{0,1}$ are the Bessel functions of the zero and first orders, respectively. Eventually, the single-spin asymmetry obtains the form

$$\begin{aligned}
 A_N(q_T, z) &= \frac{2q_T q_L \sqrt{z} \sum_X |\phi_0(q_T, z)| |\phi_s(q_T, z)|}{zq_L^2 \sum_X |\phi_0(q_T, z)|^2 + q_T^2 \sum_X |\phi_s(q_T, z)|^2} \\
 &\times \sin(\delta_s - \delta_0),
 \end{aligned}
 \tag{18}$$

where

$$\tan \delta_{0,s} = \frac{\operatorname{Im} \phi_{0,s}(q_T, z)}{\operatorname{Re} \phi_{0,s}(q_T, z)}.
 \tag{19}$$

The parameter-free calculations agree with the PHENIX experiment data [18,19], as demonstrated in Figure 3.

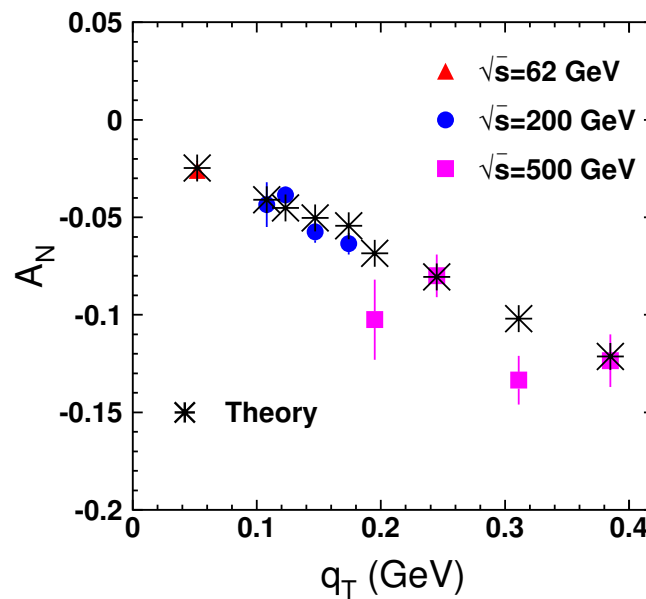


Figure 3. The single-spin asymmetry, A_N , in the polarized $pp \rightarrow nX$ process at the centre-of-mass energy $\sqrt{s} = 200$ GeV versus neutron transverse momentum q_T . The data points from Refs. [18,19] are self-explanatory, and the stars show the results of the parameter-free calculations with proper kinematics [13].

5. Polarized pA Collisions

5.1. The Cross Section

5.1.1. Glauber Approximation

A natural extension of Equation (1) to nuclear targets has the form

$$\begin{aligned}
 \frac{d\sigma(pA \rightarrow nX)}{d \ln(z) dq_T^2 d^2b_A} &= f_{\pi/p}(z, q_T) \\
 &\times \int \frac{d\sigma_{\text{tot}}^{\pi A}(M_X^2)}{d^2b_A} S_{NA}(b_A),
 \end{aligned}
 \tag{20}$$

where b_A is the impact parameter of pA collision, and $S_{NA}(b_A)$ is the additional nuclear absorption factor described below.

This expression can be interpreted as an interaction of the projectile Fock component, $|\pi^+ n\rangle$, with the target, whereby the proton light-cone momentum in the respective fractions of z and $(1 - z)$ are shared. While the pion interacts inelastically with the target, the spectator neutron has to remain intact, i.e., it has to survive its passage through the nucleus.

The partial total pion-nucleus cross section in Equation (20) can be evaluated in the Glauber approximation [22,23]

$$\left. \frac{\sigma_{\text{tot}}^{\pi A}(M_X^2)}{d^2b_A} \right|_{\text{Gl}} \approx 2 \left[1 - e^{-\frac{1}{2} \sigma_{\text{tot}}^{\pi N}(M_X^2) T_{\pi A}(b_A)} \right]. \tag{21}$$

Here,

$$T_{\pi A}(b_A) = \int d^2\Delta f_{\pi N}(\Delta) T_A(\vec{b}_A - \vec{\Delta}), \tag{22}$$

where $T_A(b_A) = \int_{-\infty}^{\infty} d\zeta \rho_A(b_A, \zeta)$, is the nuclear thickness function, and $\rho_A(b_A, \zeta)$ is the nuclear density that is used in calculations in the Woods-Saxon form. The normalized partial pion-nucleon elastic amplitude is approximated by the Gaussian form

$$f_{\pi N}(\Delta) = \frac{1}{2\pi B_{\text{el}}^{\pi N}} e^{-\Delta^2/2B_{\text{el}}^{\pi N}}, \tag{23}$$

where the elastic slope rises with energy that is approximately expressed as $B_{\text{el}}^{\pi N}(s_{\pi N}) = B_0 + 2\alpha'_{\text{p}} \ln(s_{\pi N}/s_0)$ with $B_0 = 6 \text{ GeV}^{-2}$, $\alpha'_{\text{p}} = 0.25 \text{ GeV}^{-2}$, $s_0 = 1 \text{ GeV}^2$ [2]. Notice that, for numerical calculations we use hereafter that are more accurate than the optical approximation form, we replaced $e^{-\frac{1}{2} \sigma_{\text{tot}}^{\pi N} T_{\pi A}} \Rightarrow [1 - \sigma_{\text{tot}}^{\pi N} T_{\pi A}/2A]^A$, where the quantity A denotes the atomic mass number.

Correspondingly, the neutron survival factor in Equation (20) reads as follows:

$$\begin{aligned} S_{NA}(b_A) \Big|_{\text{Gl}} &\approx \frac{e^{-\sigma_{\text{in}}^{nN}(zs) T_{NA}(b_A)} - e^{-\sigma_{\text{in}}^{pN}(s) T_{NA}(b_A)}}{T_{NA}(b_A) [\sigma_{\text{in}}^{pN}(s) - \sigma_{\text{in}}^{nN}(zs)]} \\ &\approx e^{-\sigma_{\text{in}}^{nN}(s) T_{NA}(b_A)}. \end{aligned} \tag{24}$$

If the nucleus remains intact or decays into fragments without particle production, then instead of the total πA cross section, which one should use in Equation (20), the diffractive cross sections related to elastic $\pi A \rightarrow \pi A$ and quasielastic $\pi A \rightarrow \pi A^*$ channels should be used instead. The corresponding cross section has the form [22,23]

$$\begin{aligned} \left. \frac{\sigma_{\text{diff}}^{\pi A}(M_X^2)}{d^2b_A} \right|_{\text{Gl}} &= \left[1 - e^{-\frac{1}{2} \sigma_{\text{tot}}^{\pi N} T_A(b_A)} \right]^2 \\ &+ \sigma_{\text{el}}^{\pi N} T_A(b_A) e^{-\sigma_{\text{in}}^{\pi N} T_A(b_A)}, \end{aligned} \tag{25}$$

where the first and second terms correspond to the elastic and quasi-elastic scatterings, respectively.

The difference between the cross sections, as in Equations (20) and (25), is related to the inelastic πA interactions, which lead to multiparticle production. Correspondingly, one should modify Equation (20) by replacing the total by inelastic πA cross section [22,23],

$$\left. \frac{\sigma_{\text{in}}^{\pi A}(M_X^2)}{d^2b_A} \right|_{\text{Gl}} = 1 - e^{-\sigma_{\text{in}}^{\pi N} T_A(b_A)} \tag{26}$$

Gribov Corrections: Color Transparency

It is known that the Glauber approximation is subject to Gribov inelastic shadowing corrections [24], which are known to make the nuclear matter more transparent for hadrons [22,25]; in addition, these corrections also affect both factors in Equation (20), as well as suppress $\sigma_{\text{tot}}^{\pi A}$ and increase $S_{NA}(b_A)$. We calculated the Gribov corrections to all of the orders of the multiple interactions by employing the dipole representation, as is described in Refs. [22,23,25,26].

Hadron wave function on the light front can be expanded over different Fock states, and they consist of parton ensembles that have the various transverse positions \vec{r}_i of the partons. The interaction cross section of such a hadron is averaged over the Fock states $\sigma_{\text{tot}}^{hp} = \langle \sigma(\vec{r}_i) \rangle_h$, where $\sigma(\vec{r}_i)$ is the cross section of the interaction of the partonic ensemble when it has the transverse coordinates \vec{r}_i with the proton target.

Notice that high-energy partonic ensembles are eigenstates of interaction [25], i.e., the parton coordinates \vec{r}_i remain unchanged during the interaction. Therefore, the eikonal approximation employed in the Glauber model (21)–(25) should not be used for hadrons. However, with respect to the Fock components, the whole exponential terms should be averaged [25,26]. This corresponds to the following replacements in Equations (21)–(25):

$$e^{-\frac{1}{2}\sigma_{\text{tot}}^{hN}T_A} = e^{-\frac{1}{2}\langle\sigma(\vec{r}_i)\rangle_h T_A} \Rightarrow \left\langle e^{-\frac{1}{2}\sigma(\vec{r}_i) T_A} \right\rangle_h, \tag{27}$$

where subscript ‘h’ indicates averaging over hadrons.

The difference between these averaging procedures can be exactly represented by the Gribov corrections [25,26].

The results of averaging in Equation (27) for the proton-nucleus interactions was calculated in Ref. [23] with a realistic saturated parameterization of the dipole cross section [27]; in addition, the quark-diquark model was used for the nucleon wave function:

$$\left\langle e^{-\frac{1}{2}\sigma(r_T)T_A} \right\rangle = e^{-\frac{1}{2}\sigma_0 T_A(b)} \sum_{n=0}^{\infty} \frac{[\sigma_0 T_A(b)]^n}{2^n (1+n\delta) n!}, \tag{28}$$

where

$$\sigma_0(s) = \sigma_{\text{tot}}^{pp}(s) \left[1 + \frac{1}{\delta} \right], \tag{29}$$

and $\delta = 8\langle r_{\text{ch}}^2 \rangle_p / 3R_0^2(s)$. We use the mean proton charge radius squared $\langle r_{\text{ch}}^2 \rangle_p = 0.8 \text{ fm}^2$ [28] and the energy-dependent saturation radius $R_0(s) = 0.88 \text{ fm} (s_0/s)^{0.14}$ with $s_0 = 1000 \text{ GeV}^2$ [27].

Gluon shadowing corrections, which correspond to the triple-Pomeron term in the context of diffraction, were also introduced [22,23].

5.2. Calculation Results

The results of the Glauber model calculations, including the Gribov corrections, are obtained for the partial inclusive cross section of $pAu \rightarrow nX$. Furthermore, Equation (20) is normalized by the $pp \rightarrow nX$ cross section, and this is shown in Figure 4 via the top solid red (RHIC) and top blue dashed (LHC) curves. The two other lower curves show the cross section of the inelastic and diffractive channels. One can see that the cross section is quite small, and this can be understood as a consequence of the significant suppression that occurred by a factor of $S_{NA}(b_A)$, as can be seen in Equation (24). Indeed, the impact parameter dependencies of the inclusive (21) and diffractive (25) cross sections of neutron production are depicted in Figure 5. One can see that neutrons are produced from the very periphery of the nucleus, and this is why the b_A -integrated cross section is so small. Correspondingly, the ratio shown in Figure 4 fell for the heavy nuclei as $A^{-2/3}$.

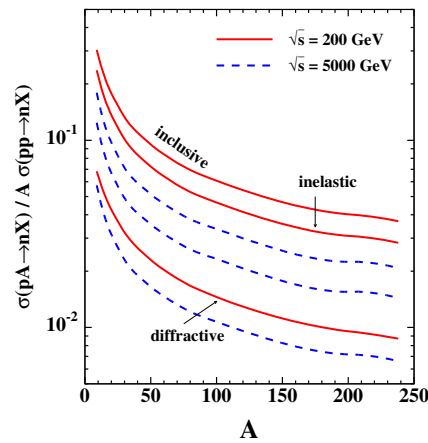


Figure 4. The pA impact parameter b_A -integrated cross sections, which are normalized by the pp cross section of the leading neutron production. The solid and dashed curves correspond to both the pAu and pPb collisions at $\sqrt{s} = 200$ GeV and 5000 GeV, respectively. The three curves in each set correspond to the inclusive, inelastic and diffractive neutron productions (top to bottom).

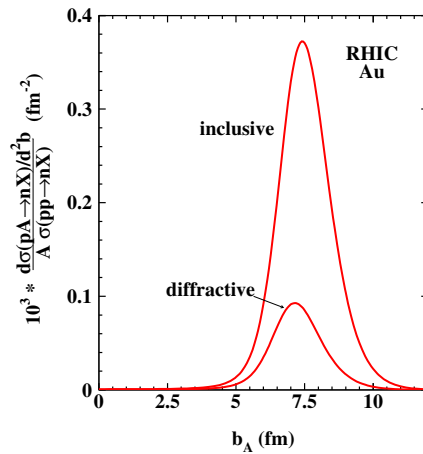


Figure 5. Partial cross sections for the inclusive and diffractive neutron production in the pAu collisions at $\sqrt{s} = 200$ GeV and $z = 0.75$.

When close to the pion pole, we treated the vertex $\pi + p \rightarrow X$, as shown in Figure 1, as the pion-proton interaction amplitude. By squaring it, one obtains the total pion-proton cross section, as was obtained in Equation (1). In the case of a nuclear target, one should replace the proton by a nucleus and obtain $\sigma_{\text{tot}}^{\pi A}(M_X^2)$. The latter obtained contributions from different channels, which can be classified as inelastic and diffractive interactions. The former corresponds to multiparticle production, which filled the rapidity interval between the colliding pion and nucleus, while the latter corresponds to the rapidity gap events. The corresponding cross sections can be evaluated with the models described below.

The recent measurements of the forward neutrons in the PHENIX experiment [16,29,30] was supplemented with beam-beam counters (BBCs), whereby the charged particles in the two pseudo-rapidity intervals of $3.0 < |\eta| < 3.9$ were detected. The results of the measurements of the forward neutrons are presented here for the different samples of events:

- (i) inclusive neutron production with the BBCs switched off;
- (ii) neutrons accompanied with multiparticle production (where one or both BBCs are fired), can be associated with inelastic πA collisions;
- (iii) if both BBCs are vetoed, a large contribution of diffractive interactions might be expected.

Notice that such a correlation with BBC activities and related processes should not be taken literally, and that a comparison with theoretical predictions should be performed with precaution. Further experimental studies employing Monte-Carlo simulations are required.

6. Glauber Model for Single-Spin Asymmetry in Polarized $pA \rightarrow nX$

Single-spin asymmetry that occurs on a nuclear target due to $\pi \tilde{a}_1$ interference can be calculated with a modified Equation (12), in which one should replace

$$\frac{d\sigma_{\pi p \rightarrow \tilde{a}_1 p}(M_X^2)/dt|_{t=0}}{d\sigma_{\pi p \rightarrow \pi p}(M_X^2)/dt|_{t=0}} \Rightarrow \frac{d\sigma_{\pi A \rightarrow \tilde{a}_1 A}(M_X^2)/dt|_{t=0}}{d\sigma_{\pi A \rightarrow \pi A}(M_X^2)/dt|_{t=0}}. \tag{30}$$

The replacement (30) leads to a single-spin asymmetry, which can be presented in the form

$$A_N^{pA \rightarrow nX} = A_N^{pp \rightarrow nX} \times \frac{R_1}{R_2} R_3. \tag{31}$$

In the ratio R_1/R_2 , R_1 corresponds to the numerator and R_2 to the denominator in the right-hand side of Equation (30). The factor R_3 is related to the experimental setup and is fixed below.

Factor R_1 , in accordance with Equations (12) and (30), is the nuclear modification factor for the forward amplitude of $\pi A \rightarrow \tilde{a}_1 A$, which is a coherent diffractive transition. In the Glauber approximation, it has the form

$$R_1 = \int d^2b_A \int_{-\infty}^{\infty} d\zeta \rho_A(b_A, \zeta) e^{-\frac{1}{2}\sigma_{\text{tot}}^{pp} T_A(b_A)} \times \exp \left[-\frac{1}{2}\sigma_{\text{tot}}^{\pi N} T_-(b_A, \zeta) - \frac{1}{2}\sigma_{\text{tot}}^{\tilde{a}_1 N} T_+(b_A, \zeta) \right], \tag{32}$$

where $T_-(b_A, \zeta) = \int_{-\infty}^{\zeta} d\zeta' \rho_A(b_A, \zeta')$ and $T_+(b_A, \zeta) = T_A(b_A) - T_-(b_A, \zeta)$.

In Equation (32), we assume that the incoming pion propagates through the nuclear thickness $T_-(b_A, \zeta)$, and that the outgoing \tilde{a}_1 propagates through $T_+(b_A, \zeta)$. Both attenuate with their corresponding cross sections. The transition occurs at the point with the longitudinal coordinate ζ , which varies from $-\infty$ to $+\infty$.

When integrating Equation (32) over ζ analytically, one arrives at

$$R_1 = \frac{1}{\Delta\sigma} \int d^2b_A e^{-\frac{1}{2}\sigma_{\text{tot}}^{\pi p} T_A(b_A)} \times \left[1 - e^{-\frac{1}{2}\Delta\sigma T_A(b_A)} \right] e^{-\frac{1}{2}\sigma_{\text{tot}}^{pp} T_A(b_A)}, \tag{33}$$

where $\Delta\sigma = \sigma_{\text{tot}}^{\tilde{a}_1 N} - \sigma_{\text{tot}}^{\pi N}$. As was mentioned above, and was explained in detail in Refs. [13,21,31], the diffractive production of the a_1 axial-vector meson is a very weak signal compared with ρ - π production, which form a rather narrow peak in the invariant mass distribution. Therefore, $\sigma_{\text{tot}}^{\tilde{a}_1 N} = \sigma_{\text{tot}}^{\rho N} + \sigma_{\text{tot}}^{\pi N}$ and $\Delta\sigma = \sigma_{\text{tot}}^{\rho N}$ have acceptable accuracy. The data for the photoproduction of the ρ meson in the nuclei agree with $\sigma_{\text{tot}}^{\rho N} \approx \sigma_{\text{tot}}^{\pi N}$; as such, we fix $\Delta\sigma$ at this value.

Nuclear modification, which corresponds to the denominator of Equation (30), is determined by Equations (20)–(24), and it has the form

$$R_2 = \frac{2}{\sigma_{\text{tot}}^{\pi p}} \int d^2b_A \left[1 - e^{-\frac{1}{2}\sigma_{\text{tot}}^{\pi p} T_A(b_A)} \right] e^{-\frac{1}{2}\sigma_{\text{tot}}^{pp} T_A(b_A)}. \tag{34}$$

The factor R_3 depends on how the measurements were conducted. If the BBCs are fired, a proper estimate would be $R_3 = \sigma_{\text{tot}}^{\pi A} / \sigma_{\text{in}}^{\pi A}$. Otherwise, if the BBC are switched off (i.e., inclusive neutron productions), we fix $R_3 = 1$. The results corresponding to these two

choices are plotted in Figure 6 by solid and dotted curves, respectively. All the data points that correspond to the events with BBCs were fired. However, the full green and open red points corresponded to events where either both BBCs fired or only one of them fired in the nuclear direction, respectively [16,29,30].

The difference between these two results reflects the uncertainty in the physical interpretation of events when there were fired with vetoed BBCs. This can be improved by applying a detailed Monte Carlo modeling. Nevertheless, the results of our calculations, as presented in Figure 6, can be reproduced reasonably well in experimental data [16,29,30].

A remarkable feature of the single-spin asymmetry A_N of the neutrons produced on nuclear targets is quite a weak A -dependence, which is seen both in the data and in our calculations. The reason for this can be understood as follows. All of the A -dependence of the A_N asymmetry is contained in the factors R_1 and R_2 in Equation (31). It turns out that the strong nuclear absorption factor $S_{NA}(b_A)$ in Equation (24) is contained in both Equations (33) and (34), and this factor pushes neutron production to the very periphery of the nucleus. This is demonstrated by the b_A -unintegrated factors $R_1(b_A)$ and $R_2(b_A)$, which are plotted in Figure 7 in gold at $\sqrt{s} = 200$ GeV. Due to the observed similarity of the A -dependencies of R_1 , R_2 , and proportional to $A^{1/3}$, they are mostly canceled in Equation (31), thereby resulting in a nearly A -independent single-spin asymmetry of neutrons.

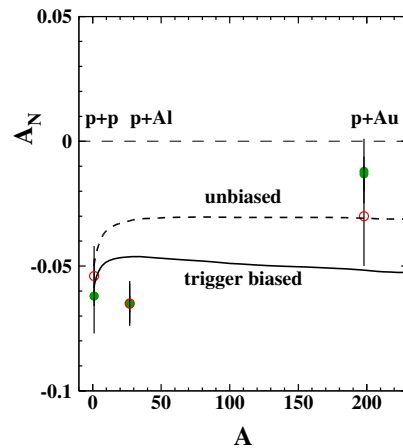


Figure 6. A_N in polarized $pA \rightarrow nX$ versus A at $\sqrt{s} = 200$ GeV, $\langle q_T \rangle = 0.115$ GeV, and $\langle z \rangle = 0.75$. The full and open data points correspond to events with either both BBCs fired or with only one of them fired in the nuclear direction, respectively [16,29,30]. An attempt to model these two classes of events is represented by the solid and dashed curves, respectively. See text for details.

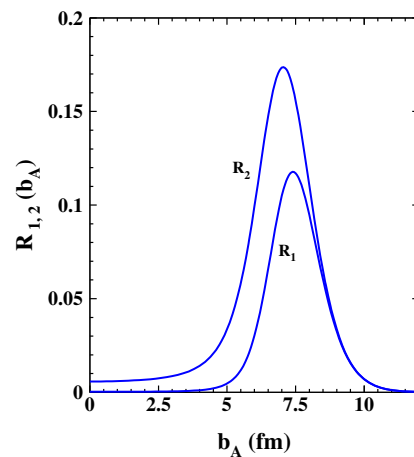


Figure 7. Impact parameter dependence of the denominator R_1 and numerator R_2 in Equation (31) according to Equations (33) and (34), respectively. Calculations are performed for neutron production in the pAu collisions at $\sqrt{s} = 200$ GeV.

7. Summary

The previously developed methods of calculation of the cross section of the leading neutron production in pp collisions were extended to nuclear targets. The nuclear absorptive corrections, as calculated in the Glauber-Gribov approach, were so strong that they pushed the partial cross sections of the leading neutron production to the very periphery of the nucleus. As a result, the A -dependencies of the inclusive and diffractive neutron production turned out to be similar, i.e., $\sim A^{1/3}$.

The mechanism of the πa_1 interference, which successfully explains the observed single-spin asymmetry in the polarized reaction $pp \rightarrow nX$, was extended to the collisions of the polarized protons with nuclei. When corrected for nuclear effects, it explained well enough the observed A_N asymmetry in inelastic events, which is when the nucleus violently breaks up [16,29,30]. However, the large value and the opposite sign of the A_N observed in the diffractive sample still remains a challenge.

Author Contributions: The authors contributed equally to this work. All authors have read and agreed to the published version of the manuscript.

Funding: This work was supported, in part, by the grants from Chilean National Agency for Research and Development (ANID)—Chile FONDECYT 1231062 and 1230391, by ANID PIA/APOYO AFB220004, and by ANID—The Millennium Science Initiative Program ICN2019_044.

Data Availability Statement: All data used in this analysis have been published in the cited publications.

Acknowledgments: We are thankful to Alexander Bazilevsky and Itaru Nakagawa for providing us with data and the details of the measurements, as well as for numerous informative discussions.

Conflicts of Interest: The authors declare no conflict of interest.

References

1. Abarbanel, H.D.I.; Gross, D.J. Spin dependence in inclusive collisions. *Phys. Rev. Lett.* **1971**, *26*, 732–734. [\[CrossRef\]](#)
2. Kopeliovich, B.Z.; Potashnikova, I.K.; Schmidt, I.; Soffer, J. Damping of forward neutrons in pp collisions. *Phys. Rev. D* **2008**, *78*, 014031. [\[CrossRef\]](#)
3. Haber, H.E.; Kane, G.L. The search for the A_1 meson. *Nucl. Phys. B* **1977**, *129*, 429–460. [\[CrossRef\]](#)
4. Flauger, W.; Mönig, F. Measurement of inclusive zero-angle neutron spectra at the CERN ISR. *Nucl. Phys. B* **1976**, *109*, 347–356. [\[CrossRef\]](#)
5. Kopeliovich, B.; Povh, B.; Potashnikova, I. Deep-inelastic electroproduction of neutrons in the proton fragmentation region. *Z. Phys. C* **1996**, *73*, 125–131. [\[CrossRef\]](#)
6. Bishari, M. Pion exchange and inclusive spectra. *Phys. Lett. B* **1972**, *38*, 510–514. [\[CrossRef\]](#)
7. Boreskov, K.G.; Grigorian, A.A.; Kaidalov, A.B. Nucleon charge exchange in inclusive reactions and the Reggeized one-pion-exchange model. *Sov. J. Nucl. Phys.* **1976**, *24*, 411–417.
8. Boreskov, K.G.; Grigorian, A.A.; Kaidalov, A.B.; Levintov, I.I. Dynamics of spin flip dynamics and inclusive processes. *Sov. J. Nucl. Phys.* **1978**, *27*, 432–438.
9. D’Alesio, U.; Pirner, H.J. Target fragmentation in pp , ep and γp collisions at high-energies. *Eur. Phys. J. A* **2000**, *7*, 109–119. [\[CrossRef\]](#)
10. Moriarty, K.J.M.; Tabor, J.H.; Ungkitchanukit, A. Absorption corrections in the inclusive production of the $\Delta(1236)$ in the triple-Regge region. *Phys. Rev. D* **1977**, *16*, 130–138. [\[CrossRef\]](#)
11. Khoze, V.A.; Martin, A.D.; Ryskin, M.G. Soft diffraction and the elastic slope at Tevatron and LHC energies: A multi-Pomeron approach. *Eur. Phys. J. C* **2000**, *18*, 167–179. [\[CrossRef\]](#)
12. Kaidalov, A.B.; Khoze, V.A.; Martin, A.D.; Ryskin, M.G. Leading neutron spectra. *Eur. Phys. J. C* **2006**, *47*, 385–393. [\[CrossRef\]](#)
13. Kopeliovich, B.Z.; Potashnikova, I.K.; Schmidt, I.; Soffer, J. Single transverse spin asymmetry of forward neutrons. *Phys. Rev. D* **2011**, *84*, 114012. [\[CrossRef\]](#)
14. Kopeliovich, B.Z.; Potashnikova, I.K.; Povh, B.; Schmidt, I. Pion structure function at small x from deep-inelastic scattering data. *Phys. Rev. D* **2012**, *85*, 114025. [\[CrossRef\]](#)
15. Kopeliovich, B.Z.; Potashnikova, I.K.; Schmidt, I.; Pirner, H.J.; Reygers, K. Pion-pion cross section from proton-proton collisions at the LHC. *Phys. Rev. D* **2015**, *91*, 054030. [\[CrossRef\]](#)
16. Aidala, C.; Akiba, Y.; Alfred, M.; Andrieux, V.; Aoki, K.; Apadula, N.; Asano, H.; Ayuso, C.; Azmoun, B.; Babintsev, V.; et al. Nuclear Dependence of the transverse-single-spin asymmetry for forward neutron production in polarized $p + A$ collisions at $\sqrt{s_{NN}} = 200$ GeV. *Phys. Rev. Lett.* **2018**, *120*, 022001. [\[CrossRef\]](#)

17. Kopeliovich, B.Z.; Potashnikova, I.K.; Schmidt, I.; Soffer, J. Leading neutrons from polarized pp collisions. *AIP Conf. Proc.* **2008**, *1056*, 199–206. [[CrossRef](#)]
18. Adare, A.; Afanasiev, S.; Aidala, C.; Ajitanand, N.N.; Akiba, Y.; Al-Bataineh, H.; Alexander, J.; Aoki, K.; Aphecetche, L.; Asai, J.; et al. Inclusive cross section and single transverse spin asymmetry for very forward neutron production in polarized $p + p$ collisions at $\sqrt{s} = 200$ GeV. *Phys. Rev. D* **2013**, *88*, 032006. [[CrossRef](#)]
19. Goto, Y.; Afanasiev, S.; Aidala, C.; Ajitanand, N.N. Inclusive cross section and single transverse-spin asymmetry of very forward neutron production at PHENIX. *Phys. Part. Nucl.* **2014**, *45*, 79–81. [[CrossRef](#)]
20. Deck, R.T. Kinematical interpretation of the first π - p resonance. *Phys. Rev. Lett.* **1964**, *13*, 169–173. [[CrossRef](#)]
21. Bel'kov, A.A.; Kopeliovich, B.Z. The Adler relation and neutrino-production of single hadrons. *Sov. J. Nucl. Phys.* **1987**, *46*, 499–505.
22. Kopeliovich, B.Z. Transparent nuclei and deuteron-gold collisions at relativistic energies. *Phys. Rev. C* **2003**, *68*, 044906. [[CrossRef](#)]
23. Kopeliovich, B.Z.; Potashnikova, I.K.; Schmidt, I. Large rapidity gap processes in proton-nucleus collisions. *Phys. Rev. C* **2006**, *73*, 034901. [[CrossRef](#)]
24. Gribov, V.N. Glauber corrections and the interaction between high-energy hadrons and nuclei. *Sov. Phys. JETP* **1969**, *29*, 483–487.
25. Zamolodchikov, A.B.; Kopeliovich, B.Z.; Lapidus, L.I. Color dynamics in hadron diffraction by nuclei. *JETP Lett.* **1981**, *33*, 595–597.
26. Kopeliovich, B.Z. Gribov inelastic shadowing in the dipole representation. *Int. J. Mod. Phys. A* **2016**, *31*, 1645021. [[CrossRef](#)]
27. Kopeliovich, B.Z.; Schäfer, A.; Tarasov, A.V. Nonperturbative effects in gluon radiation and photoproduction of quark pairs. *Phys. Rev. D* **2000**, *62*, 054022. [[CrossRef](#)]
28. Rosenfelder, R. Coulomb corrections to elastic electron-proton scattering and the proton charge radius. *Phys. Lett. B* **2000**, *479*, 381–386. [[CrossRef](#)]
29. Bazilevsky, A. RHIC Spin Program: Highlights, Recent Results and Future Opportunities. Talk at the 6th International Workshop on High Energy Physics in the LHC Era, Valparaiso, Chile, 6–12 January 2016. Available online: <https://indico.cern.ch/event/385771/contributions/919163/> (accessed on 14 October 2023).
30. Nakagawa, I. The first transverse single spin measurement in high energy polarized proton-nucleus collision at the PHENIX experiment at RHIC. *J. Phys. Conf. Ser.* **2016**, *736*, 012017. [[CrossRef](#)]
31. Kopeliovich, B.Z.; Potashnikova, I.K.; Schmidt, I.; Siddikov, M. Breakdown of partial conservation of axial current in diffractive neutrino interactions. *Phys. Rev. C* **2011**, *84*, 024608. [[CrossRef](#)]

Disclaimer/Publisher's Note: The statements, opinions and data contained in all publications are solely those of the individual author(s) and contributor(s) and not of MDPI and/or the editor(s). MDPI and/or the editor(s) disclaim responsibility for any injury to people or property resulting from any ideas, methods, instructions or products referred to in the content.